que normal au plan des couches. Cet assemblage engendre des canaux parallèles à [010] qui sont limités par des faces d'octaèdres $CdCl_6$ et des faces de polyèdres $KCl_7(H_2O)_2$ dont deux sommets sont occupés par des molécules d'eau. Dans le composé anhydre, les couches de polyèdres KCl_9 sont reliées entre elles à la fois par des arêtes communes à des polyèdres KCl_9 et par des chaînes doubles d'octaèdres $CdCl_6$ dont la plus grande dimension de section est appliquée contre les couches. Ainsi, on trouve que dans la structure du composé anhydre, par comparaison avec celle de l'hydrate, il y a dans chaque couche et par période [010], un sommet de plus d'octaèdre de double chaîne $CdCl_6$ partagé par chaque polyèdre de coordination du potassium. Cet arrangement permet au cadmium et au potassium d'avoir les mêmes indices de coordination dans les deux structures où le rapport du nombre de cations au nombre d'anions est inchangé. En outre les canaux [010] limités par Cl et H_2O que l'on observe dans l'hydrate n'existent pas dans $KCdCl_3$.

Les deux structures $KCdCl_3.H_2O$ et $KCdCl_3$ présentent donc des ensembles d'atomes disposés de manière identique. Ce sont ceux qui dans le composé hydraté correspondent à chaque couche (001) des polyèdres de coordination du potassium et aux chaînes simples d'octaèdres $CdCl_6$ en contact avec les deux faces de la couche. La Fig. 3 et le Tableau 2 illustrent et précisent les correspondances structurales remarquables qui existent entre les deux composés et expliquent la croissance orientée de l'un par rapport à l'autre.

Références

HÉRING, H. (1936). *Ann. Chim. (Paris)*, **5**, 483–586.
LECLAIRE, A. & MONIER, J. C. (1982). *Acta Cryst.* B**38**, 724–727.
LEDÉSERT, M. & MONIER, J. C. (1983). *Z. Kristallogr.* Accepté.

Acta Cryst. (1984). B**40**, 76–82

Real Structure of Undoped Y_2O_3 Single Crystals

BY FRANTIŠEK HANIC

Institute of Inorganic Chemistry, Chemical Research Centre, Slovak Academy of Sciences, 84236 *Bratislava, Czechoslovakia*

MÁRIA HARTMANOVÁ

Institute of Physics, Electro-Physical Research Centre, Slovak Academy of Sciences, 84228 *Bratislava, Czechoslovakia*

AND GALINA G. KNAB, AIDA A. URUSOVSKAYA AND KHACHIK S. BAGDASAROV

Institute of Crystallography, Academy of Sciences of the USSR, 117333 *Moscow, USSR*

(*Received* 24 *January* 1983; *accepted* 21 *October* 1983)

Abstract

Undoped Y_2O_3 single crystals (bixbyite-type structure) were grown in metallic tubes by a vertically oriented crystallization technique. The samples obtained are characterized by the lattice parameter of 10·600 (3) Å and dislocation density of the order 10^5 cm^{-2}. A detailed crystal-chemical analysis of the bixbyite structure $[^{VI}A_2][^{IV}O_3]$ allows determination of the coordinates of the A^{3+} and O^{2-} ions in bixbyite-type compounds and in their solid solutions. Some applications of the crystal-chemical analysis are described.

Introduction

The Y_2O_3 structure belongs to the bixbyite type $[^{VI}A_2][^{IV}O_3]$, which is body-centred cubic, space group $Ia3$, $Z = 16$ (Pauling & Shappel, 1930). The lattice parameter determined by neutron diffraction is 10·604 (2) Å at 300 K (O'Connor & Valentine, 1969). The Y^{3+} ions occupy the 8(*b*) ($\frac{1}{4}, \frac{1}{4}, \frac{1}{4}$) and 24(*d*) ($x, 0, \frac{1}{4}$) Wyckoff positions, and O^{2-} the 48(*e*) general positions. This structure can be related to the fluorite structure (CaF_2). An eightfold coordination of A^{2+} cations in the form of a cube in fluorite is reduced to a lower sixfold coordination of A^{3+} cations in the

0108-7681/84/020076-07$01.50 © 1984 International Union of Crystallography

bixbyite-type structure. This transition is realized in such a way that two of the eight positions of the coordination cube remain unoccupied (Sawyer, Hyde & Le Roy Eyring, 1965; Le Roy Eyring & Holmberg, 1963; Gaboriaud, 1981). However, the two unoccupied positions around A^{3+} cations in 8(*b*) are along the body diagonal, while the unoccupied positions around A^{3+} in 24(*d*) are along the face diagonal. The O^{2-} anions are surrounded tetrahedrally by four A^{3+} cations (Fig. 1). The Y^{3+} ions can be considered (Gaboriaud, 1981) to be situated at the centres of slightly deformed cubes, in which six out of eight corners are occupied by O^{2-} ions (Fig. 1).

The aims of the present study are to grow undoped Y_2O_3 single crystals, to determine their dislocation density and lattice parameter and to predict theoretically the coordinates of atoms in compounds with the bixbyite-type structure and in their solid solutions.

Experimental results and discussion

Crystal growth

The Y_2O_3 single crystals were grown in metallic tubes (W, Mo) by means of a vertically oriented crystallization technique in the apparatus developed in the Institute of Crystallography, Moscow. The crystal growth was performed at a growth rate of 2 mm h^{-1} in an argon atmosphere. The temperature gradient in the crystallization zone was 10 K cm^{-1}. The temperature during the crystallization process was kept within the limit ±0·5 K. Crystals grown in the W tube had a brown colour, which disappeared after annealing in air at 1673 K. Crystals grown in Mo tubes had a light-green colour.

The impurity content of the Y_2O_3 single crystals was determined by X-ray-fluorescence analysis. The main contamination of undoped Y_2O_3 crystals was Mg, Al, Fe, and Si within the limits of 10^{-3}–10^{-4} wt%.

Measurement of lattice parameter

The lattice parameter was measured from single crystals by Weissenberg and precession photographs using the Cu $K\alpha$ and Mo $K\alpha$ X-rays. The value obtained was 10·600 (3) Å.

The lattice parameter calculated by means of relation (18) is

$$a = (755{\cdot}4r[^{VI}Y^{3+}]^3 + 641{\cdot}3)^{1/3}$$
$$= (755{\cdot}4 \times 0{\cdot}9^3 + 641{\cdot}3)^{1/3}$$
$$= 10{\cdot}603 \text{ Å},$$

where $r[^{VI}Y^{3+}]$ is taken from Shannon (1976). This value is in good agreement with the experimental data determined by us and other authors (see Table 1).

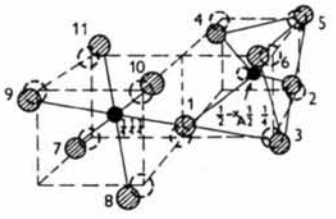

Fig. 1. Cation coordination in 8(*b*) $(\frac{1}{4},\frac{1}{4},\frac{1}{4})$ and 24(*d*) $(\frac{1}{2}-x_A,\frac{1}{2},\frac{1}{4})$ sites in the bixbyite *C*-type cubic rare-earth sesquioxide structure. Filled circles represent cations, hatched circles anions. (1) z, x, y; (2) $1-x,\frac{1}{2}+y,\frac{1}{2}-z$; (3) $\frac{1}{2}+y, z,\frac{1}{2}-x$; (4) $z, 1-x,\frac{1}{2}-y$; (5) $\frac{1}{2}+y, 1-z, x$; (6) $1-x,\frac{1}{2}-y, z$; (7) $\frac{1}{2}-x,\frac{1}{2}-y,\frac{1}{2}-z$; (8) $\frac{1}{2}-y,\frac{1}{2}-z,\frac{1}{2}-x$; (9) $\frac{1}{2}-z,\frac{1}{2}-x,\frac{1}{2}-y$; (10) x, y, z; (11) y, z, x.

Dislocation density

Samples for the investigation of dislocation density and distribution were prepared by cleaving Y_2O_3 single crystals along the {111} cleavage planes. The dislocations on the {111} planes were revealed by chemical etching in boiling 35–38% HCl for 4–5 min (as in Brower & Farabaugh, 1970). The etch pits obtained have the form of triangular pyramids, the sides being parallel to the ⟨110⟩ direction (Fig. 2). The mean dislocation density was about 10^5 cm^{-2}. The dislocation density of the best crystals prepared by the floating-zone method was 2×10^4–10^5 cm^{-2}

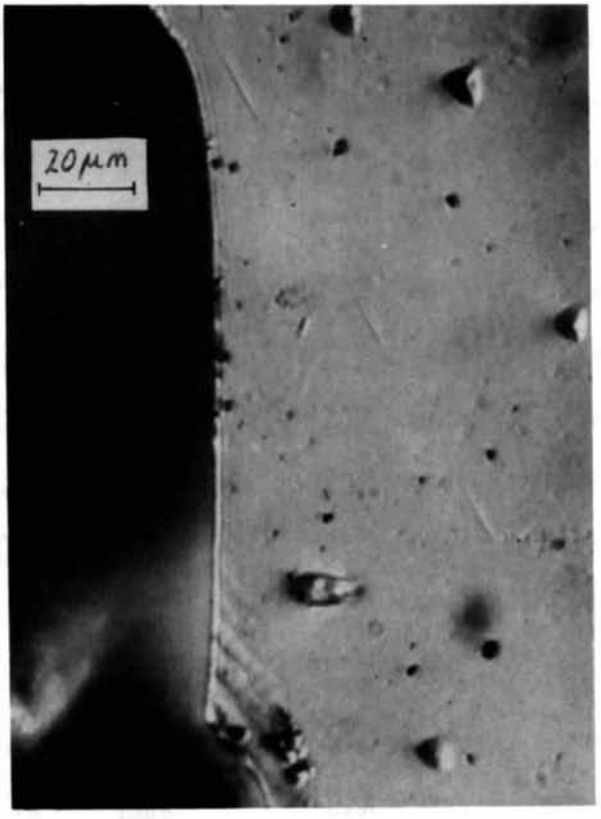

Fig. 2. Selective etching pattern of cleavage plane {111} of the Y_2O_3 crystals; etched by boiling HCl (magnification 630×).

Table 1. *Observed and calculated unit-cell parameters a [equation (18)], positional parameters x_A, x_O, y_O, z_O [equations (8), (14)–(17)] and densities ρ [equation (24)] of the bixbyite C-type sesquioxides*

Calculated values for each compound are functions of the single parameter r_A [ionic radius taken from Shannon (1976)]. n is the number of observed a_{obs} values available for evaluation of the weighted average. The positional parameters marked with an asterisk were not available experimentally, and were taken from the lattice-energy-minimization calculations of Gashurov & Sovers (1970).

Compound	r_A (Å)	$\frac{a_{obs}}{a_{calc}}$ (Å)	n	$\frac{(x_A)_{obs}}{(x_A)_{calc}}$	$\frac{(x_O)_{obs}}{(x_O)_{calc}}$	$\frac{(y_O)_{obs}}{(y_O)_{calc}}$	$\frac{(z_O)_{obs}}{(z_O)_{calc}}$	$\frac{\rho_{obs}}{\rho_{calc}}$ ($Mg\ m^{-3}$)	Reference
Y_2O_3	0·900	10·602 (7) 10·603	15	−0·0327 (3) −0·0204	0·3907 (3) 0·3811	0·1520 (3) 0·1401	0·3804 (3) 0·3794	5·015 5·032	(*a*), (*b*)
Sc_2O_3	0·745	9·846 (18) 9·843	18	−0·0351 (2) −0·0127	0·3928 (7) 0·3786	0·1528 (7) 0·1345	0·3802 (7) 0·3779	3·860 3·841	(*a*), (*c*)
β-Mn_2O_3	0·645	9·412 (8) 9·450	20	−0·0347 (8) −0·0316	0·378 (1) 0·3852	0·167 (1) 0·1485	0·397 (1) 0·3810	4·965 4·969	(*a*), (*d*)
In_2O_3	0·800	10·122 (10) 10·092	5	−0·0334 (1) −0·0116	0·3909 (12) 0·3782	0·1544 (11) 0·1336	0·3814 (13) 0·3777	7·04 7·175	(*a*), (*e*)
La_2O_3	1·032	11·37 (4) 11·374	4	— —	— —	— —	— —	— 5·882	(*a*)
Pr_2O_3	0·990	11·147 (8) 11·118	5	−0·0290 —	0·385 —	0·155 —	0·382 —	— 6·375	(*a*), (*f*)
Nd_2O_3	0·983	11·074 (14) 11·076	10	−0·0330* —	0·3900* —	0·1519* —	0·3807* —	6·49 6·578	(*a*), (*g*)
Pm_2O_3	0·970	10·99 (1) 10·999		— −0·0409	— 0·3891	— 0·1556	— 0·3818	— 6·827	(*a*)
Sm_2O_3	0·958	10·920 (16) 10·929	10	−0·0329* −0·0352	0·3899* 0·3867	0·1518* 0·1512	0·3807* 0·3814	7·205 7·096	(*a*), (*g*)
Eu_2O_3	0·947	10·859 (13) 10·865	10	−0·0330* −0·0313	0·3900* 0·3851	0·1519* 0·1483	0·3807* 0·3809	6·985 7·287	(*a*), (*g*)
Gd_2O_3	0·938	10·809 (9) 10·814	13	−0·0332* −0·0286	0·3902* 0·3841	0·1522* 0·1463	0·3807* 0·3806	7·605 7·614	(*a*), (*g*)
Tb_2O_3	0·923	10·729 (17) 10·729	5	−0·0328* −0·0248	0·3898* 0·3827	0·1517* 0·1435	0·3808* 0·3801	— 7·868	(*a*), (*g*)
Dy_2O_3	0·912	10·667 (3) 10·668	10	−0·028 −0·0225	0·387 0·3818	0·148 0·1418	0·378 0·3797	8·12 8·160	(*a*), (*h*)
Ho_2O_3	0·901	10·606 (3) 10·608	7	−0·027 −0·0205	0·388 0·3811	0·152 0·1403	0·382 0·3794	8·31 8·408	(*a*), (*d*)
Er_2O_3	0·890	10·548 (10) 10·548	8	−0·0330 −0·0188	0·394 0·3805	0·149 0·1390	0·380 0·3791	8·65 8·657	(*a*), (*d*)
Tm_2O_3	0·880	10·485 (5) 10·495	7	−0·033 −0·0174	0·392 0·3801	0·153 0·1379	0·377 0·388	8·485 8·867	(*a*), (*h*)
Yb_2O_3	0·868	10·432 (9) 10·432	12	−0·0336 −0·0159	0·391 0·3796	0·151 0·1368	0·380 0·3785	9·17 9·221	(*a*), (*d*)
Lu_2O_3	0·861	10·391 (3) 10·395	10	−0·0330* −0·0152	0·3900* 0·3793	0·1519* 0·1363	0·3807* 0·3784	9·41 9·410	(*a*), (*g*)
Tl_2O_3	0·885	10·5403 (5) 10·5317	1	— −0·0180	— 0·3803	— 0·1384	— 0·3789	10·038 10·416	(*i*)
Cm_2O_3	0·97	11·01 (2) 10·999	1	— −0·0409	— 0·3891	— 0·1556	— 0·3818	— 10·820	(*a*)
Bk_2O_3	0·96	10·889 (3) 10·940		— −0·0360	— 0·3870	— 0·1519	— 0·3814	— 10·820	(*a*)
Cf_2O_3	0·95	10·838 (3) 10·883	1	— −0·0322	— 0·3855	— 0·1490	— 0·3810	— 11·253	(*a*)

References: (*a*) *Landolt–Börnstein* (1975); (*b*) O'Connor & Valentine (1969); (*c*) Geller, Roma & Remeika (1967, 1968); (*d*) Fert (1962); (*e*) Marezio (1966); (*f*) Eyring & Baenziger (1962); (*g*) Gashurov & Sovers (1970); (*h*) Hase (1963); (*i*) Scatturin & Tornati (1953).

depending on the crystal position (Tsuiki, Kitazawa, Masumoto, Shiroki & Fueki, 1980). Subgrain boundaries were present and had an irregular form (Fig. 3). On the cleaved planes, cleavage steps were observed originating from defects (Fig. 4). It can be seen in Fig. 4 that the defects produce flat-bottom etch pits from which the cleavage steps spread in different directions. They can have a regular or an irregular form.

Crystal chemistry of the bixbyite-type structures

Determination of the coordinates of the atoms

The atomic coordinates x_A; x_O, y_O, z_O in the unit cell were derived as follows.

(1) The positional coordinate of the A^{3+} ion, x_A, results from the condition that the average interionic distance between A^{3+} and O^{2-} ions, d_{AO}, in the tetrahedron A_4O is equal to the sum of the ionic radii $r_A + r_O$ and the average angle φ is 109° 28′. The average edge length in the A_4O tetrahedron $\langle D_{AA} \rangle$ is given by the relation (Fig. 5):

$$\langle D^2_{AA} \rangle = 2d^2_{AO}[1 - \cos(109° 28')]. \quad (1)$$

The following relationships for the lengths of the six edges of the A_4O tetrahedron result from the equivalent positions of the A^{3+} ions:

$$(D^2_{AA})_{1-2,1-3} = a^2(x^2_A + \tfrac{1}{2}x_A + \tfrac{1}{8}) \quad (2)$$

$$(D^2_{AA})_{2-3,3-4} = a^2(2x^2_A + \tfrac{1}{2}x_A + \tfrac{1}{8}) \quad (3)$$

$$(D^2_{AA})_{2-4} = a^2(2x^2_A - \tfrac{1}{2}x_A + \tfrac{1}{8}) \quad (4)$$

$$(D^2_{AA})_{1-4} = a^2(x^2_A - \tfrac{1}{2}x_A + \tfrac{1}{8}) \quad (5)$$

$$\langle D^2_{AA} \rangle = \frac{a^2}{6}(9x^2_A + x_A + \tfrac{3}{4}). \quad (6)$$

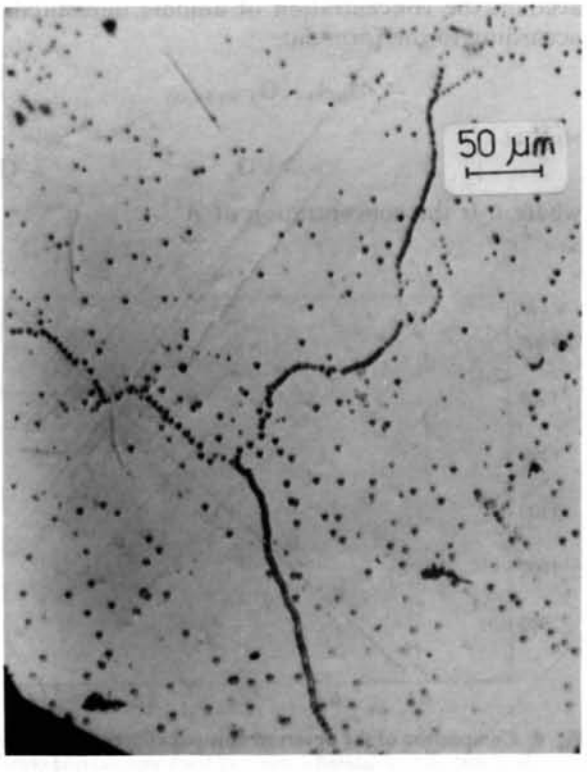

Fig. 3. Selective etching pattern of cleavage plane {111} revealing the subgrain boundaries (magnification 200×).

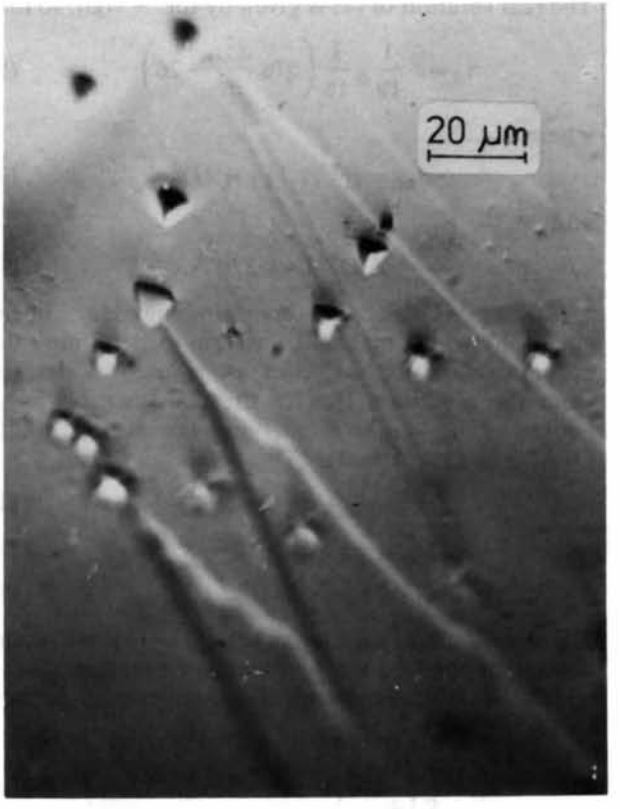

Fig. 4. The cleavage steps on the {111} plane originating from the defects on which the flat bottoms of the etch pits were formed (magnification 630×).

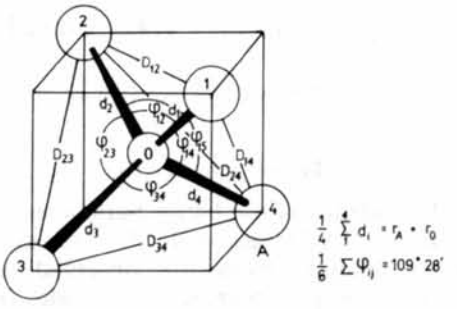

Fig. 5. Scheme of the O^{2-} anions surrounded by tetrahedral cations A in the bixbyite-type structure; D_{ij} are the tetrahedral edge lengths and d_i the distances of the tetrahedron centre from its vertices.

From equations (1) and (6) results

$$9x_A^2 + x_A + \tfrac{3}{4} - \frac{16d_{AO}^2}{a^2} = 0 \qquad (6a)$$

which gives two solutions, *i.e.* $(x_A)_{1,2}$.

The coordinate of the A^{3+} cation as a function of d_{AO} and the lattice parameter a is determined by solving equation (6*a*):

$$(x_A)_{1,2} = \frac{1}{18}\left\{-1 \pm \left[1 - 36\left(\frac{3}{4} - \frac{16d_{AO}^2}{a^2}\right)\right]^{1/2}\right\}. \qquad (7)$$

The real solution of (7) is given by the + sign, so that

$$x_A = -\frac{1}{18} + \frac{1}{18}\left(576\frac{d_{AO}^2}{a^2} - 26\right)^{1/2}, \qquad (8)$$

where

$$d_{AO} = r[^{VI}A^{3+}] + r[^{IV}O^{2-}] \qquad (9)$$

and

$$r[^{IV}O^{2-}] = 1{\cdot}370\ \text{Å}. \qquad (10)$$

(2) The system of three independent linear equations which makes it possible to determine the coordinates of the O^{2-} ions x_O, y_O, z_O was derived from the condition that in the coordination polyhedron AO_6, $\langle d_{AO}\rangle = r_A + r_O$ and the average angle O–*A*–O is approximately 90°:

$$x_O = \tfrac{1}{2} - y_O + 2x_A(2z_O - 1 - 2y_O) \qquad (11)$$

$$y_O = x_A - \tfrac{1}{4} + 2x_A(2x_O - x_A - 1) \qquad (12)$$

$$z_O = \tfrac{1}{4} + y_O + 2x_A(x_A + 2y_O). \qquad (13)$$

The simultaneous solution of (8), (11)–(13) gives coordinates of the O^{2-} ion by means of polynomials, in which the only unknown is the parameter x_A defined by (8):

$$x_O = \frac{1}{S}\left(\frac{3}{4} + x_A - 2x_A^2 - 24x_A^3 - 32x_A^4\right) \qquad (14)$$

$$y_O = \frac{1}{S}\left(\frac{1}{4} - x_A - 6x_A^2 + 8x_A^3 + 32x_A^4\right) \qquad (15)$$

$$z_O = \frac{1}{S}\left(\frac{3}{4} + x_A - 10x_A^2 - 24x_A^3 + 32x_A^4\right) \qquad (16)$$

$$S = 2 + 4x_A - 16x_A^2 - 64x_A^3. \qquad (17)$$

Determination of lattice parameter a

The dependence of the lattice parameter a on the ionic radius $r[^{VI}A^{3+}]$ (Shannon, 1976) was derived by regression analysis from the observed unit-cell dimensions of the 22 bixbyite-type oxides listed in Table 1.

The following regression equation is obtained:

$$a^3 = \{755{\cdot}4(0{\cdot}2)r[^{VI}A^{3+}]^3 + 641{\cdot}3\}\ \text{Å}^3 \qquad (18)$$

and the standard deviation of a^3, σ_V, is 6·9 Å^3. The correlation coefficient is 0·999.

Fig. 6 illustrates the dependence of the unit-cell volumes on $r[^{VI}A^{3+}]^3$. The calculated values $V = a^3$ [equation (18)] are represented by the full-line curve; the experimental values are shown by small circles. The agreement is very good. The numerical values of a_{obs} and a_{calc} [equation (18)] are given in Table 1. The reliability factor $\sum \Delta V / \sum V$ is 0·0035 for 22 compounds.

Determination of atomic coordinates and lattice parameters of solid solutions

The application of relations (8), (9), (14)–(18) makes it possible to evaluate the coordinates of ions and the unit-cell volume from the chemical composition. In the case of an isovalent solid solution it is necessary to take into account the proportion of substitutional A^{3+} and A'^{3+} cations. For the composition $A_uA'_{1-u}O_{1\cdot5}$ the effective ionic radius is

$$r_{eff} = ur[^{VI}A^{3+}] + (1-u)r[^{VI}A'^{3+}]. \qquad (19)$$

In the case of the heterovalent substitution of A^{4+} for A^{3+}, interstitial O^{2-} anions are introduced into the structure and occupy some free positions in the (cube-like) coordination polyhedra. The last term of (18) is related to the anionic dimensions and it is necessary to correct it by the factor which takes into account the concentration of anionic interstitials w according to the formula:

$$A_uA_{1-u}O_{1\cdot5(1+u/3)}$$

so that

$$w = u/3, \qquad (20)$$

where u is the concentration of A^{4+}.

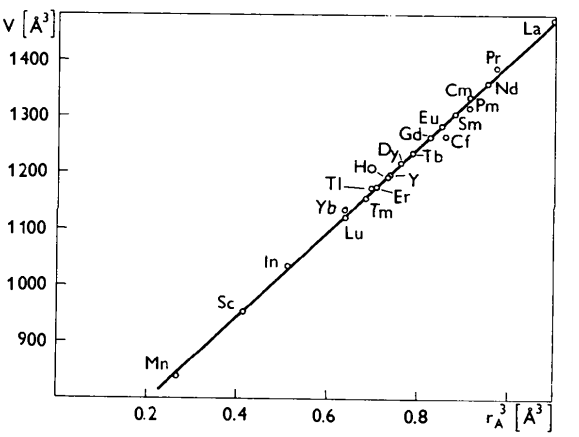

Fig. 6. Comparison of the observed unit-cell volumes (small open circles), with the calculated curve (full line) representing correlation between the unit-cell volume V and $r[^{VI}A^{3+}]^3$, from the regression analysis.

The factor by which it is necessary to correct the last term of (18) is the multiplier

$$\frac{3+u}{3}. \tag{21}$$

Then the lattice parameter of the solid solution is given by

$$a_{ss}^3 = \left[755{\cdot}4r_{eff}^3 + 641{\cdot}3\left(\frac{3+u}{3}\right)\right] \text{Å}^3. \tag{22}$$

The upper limit of stability of the bixbyite-type structure results from the condition of minimum space filling of the unit cell by A and O ions, which is, by analogy with the fluorite-type structure, 46·7%.

The space-filling coefficient Φ is defined by

$$\Phi = \frac{16(4/3)\pi[2r_A^3 + 3r_O^3]}{755{\cdot}4r_A^3 + 641{\cdot}3} \tag{23}$$

and $r_A \leq 0{\cdot}998$ Å results from the condition $\Phi \geq 0{\cdot}467$. If the value $\Phi_{max} = 0{\cdot}63$ is accepted by analogy with the fluorite-type structure, the minimum cation radius for the stable structure is 0·691 Å. It is interesting to note that (8) imposes on r_A limitations which are comparable with these values for $(r_A)_{min}$ and $(r_A)_{max}$. According to (8), only those values of r_A are acceptable which give $576d_{AO}^2/a^2 \geq 26$, so that $0{\cdot}619 < r_A < 0{\cdot}982$ Å. In the case of an ionic radius lower than 0·62–0·69 Å, the compound adopts the corundum-type structure and in the case of an ionic radius larger than 0·98–1·00 Å it transforms into the A–A_2O_3 hexagonal-type structure. The sesquioxides of La, Ce, Pr and Nd have as their stable form the hexagonal A type, in which the cation is seven coordinated [$r_{La^{3+}} = 1{\cdot}03$ Å, $r_{Ce^{3+}} = 1{\cdot}01$ Å, $r_{Pr^{3+}} = 0{\cdot}99$ Å, $r_{Nd^{3+}} = 0{\cdot}983$ Å (Shannon, 1976)]. The smallest cationic radius occurs in Mn_2O_3 ($r_{Mn^{3+}} = 0{\cdot}645$ Å). All these compounds exhibit polymorphism: La_2O_3, Ce_2O_3, Pr_2O_3, Nd_2O_3 A and C (bixbyite type) forms, Mn_2O_3 C and corundum forms (Mn_2O_3 forms solid solutions with Ti and Sn).

Some conclusions can be drawn from the above crystal-chemical analysis:

(1) The stability field of A_2O_3 bixbyite oxides becomes narrower with increasing temperature. Compounds with larger cations (La^{3+}, Nd^{3+}, Pr^{3+}) transform by heating into the hexagonal A type or the monoclinic B type at a lower temperature than compounds with smaller cations (Fig. 7). This fact can be interpreted as due to the effective radii of cations increasing more rapidly on heating than the effective anionic dimensions. The critical ratio $r_{cation}/r_{anion} = 0{\cdot}72-0{\cdot}73$ is reached at a higher temperature for smaller cations than for larger ones. Therefore the temperature stability of cubic bixbyite structures such as La_2O_3, Ce_2O_3, Nd_2O_3, Pr_2O_3 may be increased by doping with smaller cations such as Yb^{3+}, Dy^{3+}, Er^{3+}, Tb^{3+}.

(2) The change in structure during the formation of solid solutions can be predicted by means of relations (8), (14)–(22), which express the influence of the ionic dimension in isomorphic substitution and the influence of valency change in heterovalent substitution on the ionic positions. The effect of interstitial anions in increasing unit-cell dimensions is expressed by relation (22); for instance an increase of unit-cell dimensions would be expected in the case of oxidation in the Pr_2O_3–PrO_2 system, and a decrease during reduction.

(3) Relations (18) and (22) allow calculation of the densities ρ_{calc} of bixbyite-type compounds from their chemical composition (molecular weight M_r) using the relation

$$\rho_{calc} = \frac{16 \times 1{\cdot}6602 \times M_r}{a_{calc}^3}. \tag{24}$$

The calculated values (Table 1) can be used to estimate the porosity of polycrystalline samples if the experimental density is known, and to determine in this way the influence of porosity on the electrical and mechanical properties.

(4) A comparison of the observed values of the lattice parameters with their values calculated as described above makes it possible to decide whether

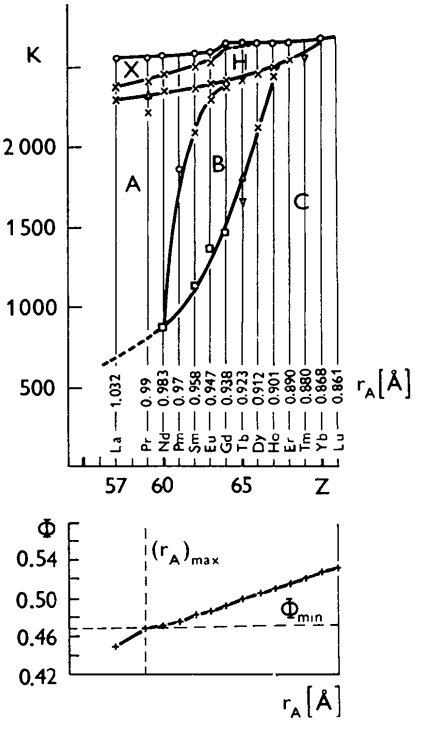

Fig. 7. Diagram of the stability fields of different forms of A_2O_3 compounds depending on temperature and ionic radius; r_A is taken from Traverse, Badie & Foex (1971); Φ is the corresponding space-filling coefficient defined as the fraction of the unit-cell volume occupied by atoms.

a solid solution or a precipitate of the coexisting phases is formed during high-temperature synthesis in the A_2O_3–A'_2O_3 or A_2O_3–$A'O_2$ systems. This is important for a correct interpretation of the measured physical properties of the system under investigation.

Determination of the concentration w of the anionic interstitials from the change in lattice parameter [equation (22)] is important in the interpretation of the physical properties of the solid solution (electrical conductivity, dielectric loss, mechanical properties) and in searching for a correlation between chemical composition and physical properties.

(5) The approximate coordinates of the ions in bixbyite-type compounds and solid solutions can be evaluated from their chemical composition using relations (8), (9), (14)–(22). The agreement between calculated and observed values is reliable (Table 1). The calculated parameters correspond to the most regular bixbyite-type model and they can be used for evaluation of approximate lattice energies.

The results of the detailed crystal-chemical analysis of the bixbyite-type compounds will be used in the investigation of materials based on Y_2O_3.

References

BROWER, W. S. JR & FARABAUGH, E. N. (1970). *J. Am. Ceram. Soc.* **53**, 225.

EYRING, L. & BAENZIGER, N. C. (1962). *J. Appl. Phys.* **33**, 428–433.

FERT, A. (1962). *Bull. Soc. Fr. Minéral. Cristallogr.* **85**, 267–270.

GABORIAUD, R. J. (1981). *Philos. Mag.* **44**, 561–587.

GASHUROV, G. & SOVERS, O. J. (1970). *Acta Cryst.* B**26**, 938–945.

GELLER, S., ROMO, P. & REMEIKA, J. P. (1967). *Z. Kristallogr.* **124**, 136–142.

GELLER, S., ROMO, P. & REMEIKA, J. P. (1968). *Z. Kristallogr.* **126**, 461.

HASE, W. (1963). *Phys. Status Solidi*, **3**, K446–K449.

Landolt–Börnstein (1975). *Zahlenwerte und Funktionen aus Naturwissenschaften und Technik* III/7. *Kristallstrukturdaten anorganischer Verbindungen.* Part b1. Berlin: Springer-Verlag.

LE ROY EYRING, B. & HOLMBERG, B. O. (1963). *Adv. Chem. Ser.* **39**, 46–54.

MAREZIO, M. (1966). *Acta Cryst.* **20**, 723–728.

O'CONNOR, B. H. & VALENTINE, T. M. (1969). *Acta Cryst.* B**25**, 2140–2144.

PAULING, L. & SHAPPEL, M. D. (1930). *Z. Kristallogr.* **75**, 128–131.

SAWYER, J. O., HYDE, B. G. & LE ROY EYRING, B. (1965). *Bull. Soc. Chim. Fr.* pp. 1190–1193.

SCATTURIN, V. & TORNATI, M. (1953). *Ric. Sci.* **23**, 1805–1813.

SHANNON, R. D. (1976). *Acta Cryst.* A**32**, 751–767.

TRAVERSE, J. P., BADIE, J. M. & FOEX, M. (1971). *Colloq. Int. CNRS*, pp. 139–147.

TSUIKI, H., KITAZAWA, K., MASUMOTO, T., SHIROKI, K. & FUEKI, K. (1980). *J. Cryst. Growth*, **49**, 71–76.

Acta Cryst. (1984). B**40**, 82–86

The Structure of $NaNb_7O_{18}$ as Deduced from HREM Images and X-ray Powder Diffraction Data

BY BENGT-OLOV MARINDER AND MARGARETA SUNDBERG

*Department of Inorganic Chemistry, Arrhenius Laboratory, University of Stockholm, S-*106 91 *Stockholm, Sweden*

(*Received* 14 *July* 1983; *accepted* 18 *October* 1983)

Abstract

A plausible crystal structure of $NaNb_7O_{18}$ has been deduced from high-resolution electron micrographs and verified by multi-slice calculations of simulated images. X-ray powder diffraction data have been used in an attempt to refine the structure. (JCPDS Diffraction File No. 34-1492). The proposed space group is *Immm*, and the unit-cell dimensions are a = 14·284 (3), b = 26·224 (4) and c = 3·8414 (6) Å, with V = 1438·9 Å^3, Z = 4, D_x = 4·437 g cm^{-3} and M_r = 961·32. The structure is related to that of $NaNb_{13}O_{33}$. Na atoms are located in the tunnels characterizing the structure but also at other sites, which provide the same coordination as the perovskite structure. Two types of structure defects, observed in the HREM images, are also presented.

Introduction

In the course of our studies on solid electrolytes we have investigated the system $NaNbO_3$–WO_3–Nb_2O_5 (Hörlin, Marinder & Nygren, 1982). It then became necessary to scrutinize the subsystem $NaNbO_3$–Nb_2O_5 in some detail. This system has been the topic of several studies, and a phase diagram has been given (Appendino, 1973). The existence of a phase found by Appendino, with the approximate composition $Na_2O.4Nb_2O_5$, isotypic with $NaNb_6O_{15}F$ (Andersson, 1965*b*), has been confirmed. Further structural details will be given elsewhere (Marinder, 1983). In this paper, however, we wish to describe another phase in the system $NaNbO_3$–Nb_2O_5, first reported by Shafer & Roy (1959) and confirmed by Appendino (1973), namely $NaNb_7O_{18}$. Some of the

0108-7681/84/020082-05$01.50 © 1984 International Union of Crystallography